The G-protein signaling regulator RGS3 enhances the GTPase activity of KRAS

Chuanchuan Li[1], **Alberto Vides**[1], **Dongsung Kim**[1], **Jenny Xue**[1,2], **Yulei Zhao**[1], **Piro Lito**[1,2,3,4,*]

[1]Human Oncology and Pathogenesis Program, Memorial Sloan Kettering Cancer, New York, NY 10065

[2]Tri-Institutional MD-PhD Program, Weill Cornell Medical College and Rockefeller University and Memorial Sloan Kettering Cancer Center, New York, NY 10065

[3]Department of Medicine, Memorial Sloan Kettering Cancer Center, New York, NY 10065

[4]Department of Medicine, Weill Cornell Medical College, New York, NY 10065

Abstract

Recently reported to be effective in patients with lung cancer, KRAS[G12C] inhibitors bind only to the inactive, or guanosine diphosphate-bound, state of the oncoprotein and require guanosine triphosphate (GTP) hydrolysis for inhibition. Yet, KRAS mutations prevent the catalytic arginine of GTPase-activating proteins (GAPs) from enhancing an otherwise slow hydrolysis rate. If KRAS mutants are indeed insensitive to GAPs, it is unclear how KRAS[G12C] hydrolyzes sufficient GTP to allow inactive state selective inhibition. Here we show that RGS3, a GAP previously known for regulating G-protein coupled receptors, can also enhance the GTPase activity of mutant and wild-type KRAS proteins. Our study reveals an unexpected mechanism that inactivates KRAS and explains the vulnerability to emerging clinically effective therapeutics.

One Sentence Summary:

RGS3 inactivates common oncogenic KRAS mutants by enhancing their guanosine triphosphate activity.

KRAS hydrolyzes guanosine triphosphate (GTP) to guanosine diphosphate (GDP) and controls diverse cellular functions by cycling between an active (GTP-bound) and an inactive (GDP-bound) conformation (1–4). Its weak intrinsic GTPase activity is enhanced by GTPase-activating proteins (GAPs) and the exchange of GDP for GTP is enhanced by guanine-nucleotide exchange factors (5–7). KRAS mutations are among the most common activating alterations found in cancer (4, 8). Most of these mutations (~80%) result in single amino acid substitutions of glycine 12 (for example, G12C/D/V/etc.) and prevent the catalytic arginine residue in GAPs from enhancing GTP-hydrolysis (3, 9, 10). Insensitivity to GAPs is thought to render KRAS oncoproteins constitutively active and independent of upstream input for activation.

Emerging evidence suggests that some KRAS oncoproteins require nucleotide exchange for activation. Perhaps the strongest evidence is provided by KRAS^{G12C} inhibitors (11–17), which selectively target the inactive state of the oncoprotein to prevent its activation by nucleotide exchange. We have previously shown that these drugs induce responses in ~1/3 of patients with lung cancer (18) and that inhibition requires an intact GTPase activity by KRAS^{G12C} (12, 17). If KRAS mutants are insensitive to GAPs, it is unclear how KRAS^{G12C} hydrolyzes sufficient GTP to allow inactive state selective inhibition.

Intrinsic hydrolysis alone may be sufficient to enable inactive state selective inhibition. To this end, we compared the rate of inhibition in cancer cells to the rate of intrinsic GTP hydrolysis by KRAS^{G12C}. The time required for maximal inhibition of KRAS in cells treated with a potent and selective G12Ci (MRTX1257, fig. S1A) ranged from ~20 min in serum-deprived medium, a condition that suppresses nucleotide exchange (half-life ~ 2 min, Fig. 1A), to ~60 min in medium with 10% serum (half-life ~ 10 min, fig. S1B). Similar cellular inhibition kinetics were observed with other potent inhibitors (k_{inac}/K_I 10 mM^{-1} s^{-1}), such as MRTX849 and AMG510 (Fig. 1A).

By comparison, purified KRAS^{G12C} hydrolyzed GTP[γ^{32}P] at a much slower rate (half-life 120–300 min, Fig. 1B and fig. S1C). The intrinsic hydrolysis half-life for KRAS proteins varies across publications (fig. S1D, range: 25–200 min). Regardless of this variation, the rate of cellular KRAS^{G12C} inhibition with potent inhibitors was quicker than even the fastest intrinsic hydrolysis estimate (19) reported in the literature (fig. S1E).

The discrepancy between the rate of cellular inactivation and the rate of the intrinsic GTPase reaction suggests the presence of cellular factors that enhance GTP-hydrolysis by KRAS^{G12C}. To test this possibility, purified KRAS was loaded with GTP[γ^{32}P] and incubated with whole-cell extracts (WCE) from lung cancer models. Because cytoplasmic RAS-GAPs, such as NF1, enhance the GTPase activity of wild-type (WT) KRAS, the latter was used as a positive control. The KRAS-nucleotide complex was immobilized and the remaining GTP[γ^{32}P] was quantified by autoradiography (hereafter referred to as the γ-phosphate assay, fig. S1C). As shown in Fig. 1C and fig. S2A, little intrinsic GTP[γ^{32}P]-hydrolysis was detected for KRAS^{G12C} at 1 h of incubation. In the presence of cellular extracts, however, there was a near complete hydrolysis of GTP[γ^{32}P] (Fig. 1C and fig. S2A). Under these conditions, the reaction reached a steady-state maximum within 2 min of incubation (Fig. 1D and fig. S2B). Cellular extracts did not affect KRAS protein stability

in these experiments (fig. S2C and D). The activity was greatly reduced in the flow-through from a 3 kDa molecular cut-off fractionation column (Fig. 1C and fig. S2A), suggesting that a cellular protein is responsible.

It has been reported that cellular extracts enhance hydrolysis by wild-type but not by mutant (G12V/D) NRAS (5). If the same holds true for KRAS^{G12C} has not been tested in the literature. In agreement with previous work, our data show that the GTPase activity of KRAS^{WT} was enhanced in a concentration dependent manner and that the effect on KRAS^{WT} was greater than on KRAS^{G12C} (fig. S2D). However, rather than being completely insensitive to cellular extracts, KRAS^{G12C} was also responsive, with activity detected at higher lysate concentrations (fig. S2D and E).

It is possible that the KRAS^{G12C} effect reflects an enhanced rate of nucleotide dissociation or the exchange of GTP for GDP. To address these possibilities, the GTPase activity of KRAS^{G12C} was assayed by loading it with GTP[α^{32}P] and subsequent incubation with cellular extracts (hereafter referred to as the α-phosphate assay, fig. S2F). Following immobilization of KRAS, the bound nucleotides were eluted and subjected to separation by thin-layer chromatography (TLC). As expected, after incubation with the GAP-related domain (GRD) of NF1, the predominant [α^{32}P]-labeled nucleotide bound to KRAS^{G12C} was GTP (Fig. 1E). By comparison, the predominant [α^{32}P]-labeled nucleotide bound to KRAS^{G12C} incubated with cell extracts was GDP. If nucleotide exchange (or nucleotide dissociation) was responsible, then GTP[α^{32}P] would be replaced with cold nucleotide and no GDP[α^{32}P] signal would be detected. Because an increase in GDP[α^{32}P] was indeed detected (Fig. 1E), the data support the presence of a cellular protein that accelerates GTP-hydrolysis by KRAS^{G12C}. Moreover, the GTPase enhancing effect of cellular extracts was attenuated when A59G — a transition state mutation that blocks GTPase activity (20) — was introduced alongside KRAS^{G12C} (fig. S2G).

To isolate the protein responsible for enhancing the GTPase activity of KRAS^{G12C}, we devised a purification scheme wherein KRAS^{G12C}-mutant cancer cell extracts (see Materials and Methods) were subjected to two rounds of size-exclusion chromatography (SEC, steps 1 and 2), desalting (step 3), anion-exchange chromatography (AEC, step 4) and mass spectrometry (MS, step 5) to identify proteins classified as GAPs (Fig. 2A). The eluted fractions from each chromatographic step were assayed for their optical density and their ability to enhance KRAS^{G12C} hydrolysis. Fractions that retained activity were pooled and carried forward to the next step. SEC step 1 elution volumes ranging from 52 to 72 mL had KRAS^{G12C}-directed GAP activity (fig. S3A). Four of these were independently subjected to SEC step 2, in order to confirm the activity and to identify which step 2 fractions to carry forward (Fig. 2B). SEC step 2 elution volumes ranging from 12 to 15 mL were pooled, desalted and analyzed by AEC with a linear salt-gradient (fig. S3B). The latter identified five peaks with KRAS^{G12C}-directed GAP activity (Fig. 2C).

The active fractions eluted in step 4 were pooled, acid-precipitated and subjected to MS in order to identify proteins annotated as GAP (fig. S3C). One of these, RGS3, is a GAP for the G$\alpha_{i/q}$ subunit of heterotrimeric G-protein coupled receptors (21–23). Many of the RGS3 peptides identified by mass spectrometry localized in the RGS domain of

the protein (RGSD, the GAP domain, fig. S3D–E). RGS3 lacks the catalytic arginine (R) residue present in canonical RAS-GAPs (24, 25). We thus reasoned that RGS3 might not be impeded by G12 mutations and decided to study it further. The broader RGS family contains 20 members (fig. S3F), which often have alternatively spliced variants. At least 9 variants of RGS3 have been reported. As expected, the 75 kDa (p75) and/or the 25 kDa (p25) RGS3 isoforms (both of which contain the RGS GAP domain) eluted in one or more fractions that enhanced GTP[γ^{32}P]-hydrolysis by KRAS^{G12C} (Fig. 2D).

In beginning to validate the effect of RGS3, we asked if it interacts with KRAS^{G12C} in cells. To this end, we relied on the ability of the G12Ci to selectively displace effector proteins from KRAS^{G12C}, while sparing those bound to wild-type KRAS, NRAS and HRAS (12, 13). Co-immunoprecipitation (IP) studies in three KRAS^{G12C}-mutant cell lines showed an interaction between endogenous KRAS^{G12C} and RGS3; an interaction that was diminished upon G12Ci-treatment (fig. S4A). GST-pulldown experiments confirmed that RGS3 interacts with either KRAS^{G12C} 4A or 4B splice variants (fig. S4B), an interaction that was less pronounced with KRAS^{WT} (fig. S4C). Direct binding assays with purified proteins suggested a preference for the active (or GTPγS-loaded) conformation of KRAS^{G12C}, as compared to the inactive (GDP-loaded) state (fig. S4D).

To directly test if RGS3 acts as a GAP for KRAS^{G12C}, we carried out GTP-hydrolysis assays with purified KRAS in the presence of RGS3 variants. In addition to the radioactive γ- and α-phosphate assays (figs. S1C and S2F), we also used a non-radioactive hydrolysis assay that enables continuous measurement of phosphate release over time (fig. S5A). As expected, RGS3 enhanced GTP-hydrolysis by KRAS^{G12C} (Fig. 3A–B and fig. S5B), leading to a concentration-dependent increase in the rate constant (fig. S5C and D). RGS3 was more effective at enhancing KRAS^{G12C} hydrolysis than canonical RAS-GAPs, such as NF1 and RASA1 (fig. S5E and F). Whereas no measurable effect was detected for RASA1, some activity was observed for NF1 (Fig. 3A–B and fig. S5E and F). The latter, however, was not significantly attenuated when the catalytic arginine of NF1 was mutated to alanine (R1276A), supporting our suspicion that KRAS^{G12C}-directed GAP activity occurs independently of the arginine residue, which is also known as the "R-finger".

Rather than having an idiosyncratic effect on KRAS^{G12C}, RGS3 also enhanced GTP-hydrolysis by G12D/V and G13C/D mutant KRAS (fig. S6A–C), which together comprise ~95% of KRAS mutations found in cancer. RGS3 also enhanced the GTPase activity of KRAS^{WT}, but in this setting RGS3 was much less effective than NF1 or RASA1 (Fig. 3A–B and fig. S5G).

RGS3 had little effect when the transition state mutation A59G was engineered alongside G12C (Fig. 3C). This suggests that RGS3 enhances hydrolysis by helping the reaction progress past the transition state. To better understand the mechanism, we constructed a molecular model using crystal structures of KRAS-GMPPNP *(6OB2, ref. 26)*, RGS3 GAP domain *(2OJ4, ref. 27)* and Ga_{ia1}-GDP·AlF$_4$:RGS4 *(1AGR, ref. 24)*. The model identified an asparagine (N) residue in the GAP domain of RGS3 as potentially involved in the hydrolysis reaction (Fig. 3D). This residue was predicted to orient away from the P-loop and, therefore, less likely to be impeded by G12 substitutions. Also, asparagine residues serve a catalytic

function in other (non RAS-specific) GAPs, including those enhancing GTP-hydrolysis by RAP1 and RHEB GTPases (28, 29).

We thus tested if the asparagine residue in RGS3 was necessary for the GTPase-activating effect on KRAS^{G12C}. A histidine (H) substitution on N460 in p75 (RGS3) or on N147 in p25 (RGSD) attenuated the effect of RGS3 proteins on GTP-hydrolysis by KRAS^{G12C}, as evidenced by the γ-phosphate (Fig. 3E) and the α-phosphate (Fig. 3F) hydrolysis assays. Because RGS3 NH mutants had some residual activity against KRAS^{G12C}, it is likely that other residues also contribute to the GAP activity. This is in agreement with reports indicating that multiple RGS residues (besides asparagine) participate in enhancing GTP hydrolysis by Gα (24). The asparagine residue is conserved between RGS isoforms, suggesting that other members of the family also enhance the KRAS GTPase activity. Indeed, this was the case for RGS4 (Fig. 3E). Together, the biochemical data suggest that RGS3 enhances the GTPase activity of KRAS in a mutant-inclusive manner (Fig. 3G).

If RGS3 enhances KRAS^{G12C}-hydrolysis it may inactivate this oncoprotein in cells. As expected, sgRNA-mediated deletion of RGS3 in KRAS^{G12C}-mutant lung cancer cells led to an increase in KRAS activation (Fig. 4A and fig. S7A). Loss of RGS3 also enhanced proliferation in culture and accelerated tumor growth in xenograft studies (Fig. 4B and fig. S7B). The proliferative advantage of RGS3$^{−/−}$ cells was largely dependent on KRAS^{G12C}, as evidenced by a previously validated (17, 30) KRAS^{G12C}-specific siRNA (fig. S7C). In agreement, siRNA-mediated knockdown of RGS3 increased proliferation in cells expressing KRAS^{G12C} but not in cells expressing KRAS$^{G12C/A59G}$ (fig. S7D), which is insensitive to the GTPase-enhancing effect of WCE (fig. S2G) or RGS3 (Fig. 3C).

To determine if RGS3 expression inversely correlated with KRAS activation in patients with lung cancer, we established a mutant KRAS-dependent transcriptional output score (fig. S8A and B) and experimentally validated its ability to detect changes in KRAS^{G12C}-driven signaling following G12Ci-treatment (fig. S8C). As shown in fig. S8D and E, a higher RGS3 expression was associated with lower mutant KRAS output in lung cancers harboring G12C or any KRAS mutation. The negative correlation was observed with distinct KRAS up-regulated or down-regulated gene expression signatures (fig. S8F and G). Little to no correlation was noted in KRAS^{WT} lung cancers.

RGS3$^{−/−}$ cells had an attenuated response to G12Ci-treatment, as compared to their isogenic RGS3 wild-type cells. This was evidenced by: 1) a diminished inhibition of KRAS-GTP levels and downstream signaling (fig. S9A, B), 2) a diminished antiproliferative effect (fig. S9C, D), and 3) a less potent antitumor effect in vivo (Fig. 4C, D and fig. S9E, F). Moreover, RGS3 expression correlated with susceptibility to G12Ci-treatment, in a panel of 9 lung cancer patient-derived xenograft (PDX) models. The PDX were established from 7 patients and their treatment response profile (fig. S10A) was similar to that reported in a recent clinical study (18). RNA sequencing (fig. S10B) and immunohistochemistry with an RGS3-specific antibody (fig. S10C, D) revealed that tumors with higher RGS3 expression had a larger magnitude of inhibition.

To provide additional evidence that RGS3 functions as a mutant KRAS-inclusive GAP, we tested the ability of RGS3-depleted extracts to directly enhance GTP[γ^{32}P]-hydrolysis by KRAS. As shown in Fig. 4E, almost complete KRAS^{G12C} hydrolysis was observed in the presence of control extracts (row 2 vs. row 1); an activity that was attenuated in RGS3$^{-/-}$ extracts (row 3). By comparison, the activity was restored in extracts from RGS3$^{-/-}$ cells expressing RGS3^{WT} (row 4) and diminished again in those expressing RGS3^{N460H} (row 5). RGS3$^{-/-}$ extracts did not significantly affect GTP[γ^{32}P] hydrolysis by KRAS^{WT} (Fig. 4F). The latter agrees with the notion that RGS3$^{-/-}$ cells still express conventional RAS-GAPs (such as NF1), which greatly enhance hydrolysis by KRAS^{WT} (Fig. 3B and fig. S5G: NF1>>RGS3), but only modestly that by KRAS^{G12C} (Fig. 3B and fig. S5E: RGS3>NF1). Lastly, the increase in cellular KRAS activation (Fig. 4G) and proliferation (Fig. 4H) conferred by the deletion of RGS3 were reversed by re-expression of RGS3^{WT}, but much less so by RGS3^{N460H}.

Here we report that the GTPase activity of KRAS is enhanced by non arginine-finger dependent GAPs, such as RGS3 (see also supplementary text). As evidenced above, RGS3 enhanced GTP hydrolysis in mutant KRAS-inclusive manner, affecting both wild-type and several oncogenic mutants (including G12C, G12D, G12V, G13C and G13D). This effect was dependent on a key asparagine residue in the GAP domain of RGS3. KRAS mutations impede the catalytic arginine (or R-finger) of canonical RAS-GAPs (such as NF1 or RASA1) from enhancing an otherwise slow GTP hydrolysis rate. If, however, KRAS mutants were completely insensitive to GAPs, then inactive state selective KRAS^{G12C} inhibitors would require a long time to take effect, when considering that the time to inhibition is limited by the rate of hydrolysis. While inhibitor potency might have hindered initial observations (13), highly-potent G12Ci inactivate the oncoprotein with minutes; quicker than even the fastest estimate of intrinsic hydrolysis rate in the literature (19). RGS3-assisted hydrolysis by KRAS^{G12C} was approximately 1–2 orders of magnitude slower than NF1- or RASA1-stimulated hydrolysis by KRAS^{WT}, suggesting that RGS3 is unlikely to inactivate the entire cellular pool of KRAS^{G12C}; that is, not to the same extent as canonical R-finger GAPs are able to do for KRAS^{WT}. As a result, KRAS^{G12C} has a longer residency time in its active (GTP-bound) conformation than KRAS^{WT}, allowing the oncoprotein to drive proliferation despite its susceptibility to 'atypical-for-RAS' GAPs (Fig. 3G). Collectively, our experiments uncover an unexpected regulatory mechanism with important implications for understanding and therapeutically targeting KRAS oncoprotein-driven cancers.

Supplementary Material

Refer to Web version on PubMed Central for supplementary material.

Acknowledgments:

References and Notes:

1. Malumbres M, Barbacid M, RAS oncogenes: the first 30 years. Nature reviews. Cancer 3, 459–465 (2003). [PubMed: 12778136]

2. Papke B, Der CJ, Drugging RAS: Know the enemy. Science 355, 1158–1163 (2017). [PubMed: 28302824]

3. Simanshu DK, Nissley DV, McCormick F, RAS Proteins and Their Regulators in Human Disease. Cell 170, 17–33 (2017). [PubMed: 28666118]

4. Li S, Balmain A, Counter CM, A model for RAS mutation patterns in cancers: finding the sweet spot. Nature reviews. Cancer 18, 767–777 (2018). [PubMed: 30420765]

5. Trahey M, McCormick F, A cytoplasmic protein stimulates normal N-ras p21 GTPase, but does not affect oncogenic mutants. Science 238, 542–545 (1987). [PubMed: 2821624]

6. Margarit SM et al. , Structural evidence for feedback activation by Ras.GTP of the Ras-specific nucleotide exchange factor SOS. Cell 112, 685–695 (2003). [PubMed: 12628188]

7. Bos JL, Rehmann H, Wittinghofer A, GEFs and GAPs: critical elements in the control of small G proteins. Cell 129, 865–877 (2007). [PubMed: 17540168]

8. Pylayeva-Gupta Y, Grabocka E, Bar-Sagi D, RAS oncogenes: weaving a tumorigenic web. Nature reviews. Cancer 11, 761–774 (2011). [PubMed: 21993244]

9. Bollag G, McCormick F, Differential regulation of rasGAP and neurofibromatosis gene product activities. Nature 351, 576–579 (1991). [PubMed: 1904555]

10. Scheffzek K et al. , The Ras-RasGAP complex: structural basis for GTPase activation and its loss in oncogenic Ras mutants. Science 277, 333–338 (1997). [PubMed: 9219684]

11. Ostrem JM, Peters U, Sos ML, Wells JA, Shokat KM, K-Ras(G12C) inhibitors allosterically control GTP affinity and effector interactions. Nature 503, 548–551 (2013). [PubMed: 24256730]

12. Lito P, Solomon M, Li LS, Hansen R, Rosen N, Allele-specific inhibitors inactivate mutant KRAS G12C by a trapping mechanism. Science 351, 604–608 (2016). [PubMed: 26841430]

13. Patricelli MP et al. , Selective Inhibition of Oncogenic KRAS Output with Small Molecules Targeting the Inactive State. Cancer Discov 6, 316–329 (2016). [PubMed: 26739882]

14. Janes MR et al. , Targeting KRAS Mutant Cancers with a Covalent G12C-Specific Inhibitor. Cell 172, 578–589 e517 (2018). [PubMed: 29373830]

15. Canon J et al. , The clinical KRAS(G12C) inhibitor AMG 510 drives anti-tumour immunity. Nature 575, 217–223 (2019). [PubMed: 31666701]

16. Hallin J et al. , The KRAS(G12C) Inhibitor MRTX849 Provides Insight toward Therapeutic Susceptibility of KRAS-Mutant Cancers in Mouse Models and Patients. Cancer Discov 10, 54–71 (2020). [PubMed: 31658955]

17. Xue JY et al. , Rapid non-uniform adaptation to conformation-specific KRAS(G12C) inhibition. Nature 577, 421–425 (2020). [PubMed: 31915379]

18. Hong DS et al. , KRAS(G12C) Inhibition with Sotorasib in Advanced Solid Tumors. N Engl J Med 383, 1207–1217 (2020). [PubMed: 32955176]

19. Hunter JC et al. , Biochemical and Structural Analysis of Common Cancer-Associated KRAS Mutations. Mol Cancer Res 13, 1325–1335 (2015). [PubMed: 26037647]

20. Hall BE, Bar-Sagi D, Nassar N, The structural basis for the transition from Ras-GTP to Ras-GDP. Proc Natl Acad Sci U S A 99, 12138–12142 (2002). [PubMed: 12213964]

21. Watson N, Linder ME, Druey KM, Kehrl JH, Blumer KJ, RGS family members: GTPase-activating proteins for heterotrimeric G-protein alpha-subunits. Nature 383, 172–175 (1996). [PubMed: 8774882]

22. Ross EM, Wilkie TM, GTPase-activating proteins for heterotrimeric G proteins: regulators of G protein signaling (RGS) and RGS-like proteins. Annu Rev Biochem 69, 795–827 (2000). [PubMed: 10966476]

23. Neubig RR, Siderovski DP, Regulators of G-protein signalling as new central nervous system drug targets. Nat Rev Drug Discov 1, 187–197 (2002). [PubMed: 12120503]

24. Tesmer JJ, Berman DM, Gilman AG, Sprang SR, Structure of RGS4 bound to AlF4--activated G(i alpha1): stabilization of the transition state for GTP hydrolysis. Cell 89, 251–261 (1997). [PubMed: 9108480]

25. Srinivasa SP, Watson N, Overton MC, Blumer KJ, Mechanism of RGS4, a GTPase-activating protein for G protein alpha subunits. J Biol Chem 273, 1529–1533 (1998). [PubMed: 9430692]

26. Rabara D et al. , KRAS G13D sensitivity to neurofibromin-mediated GTP hydrolysis. Proc Natl Acad Sci U S A 116, 22122–22131 (2019). [PubMed: 31611389]

27. Rezabkova L et al. , 14–3-3 protein interacts with and affects the structure of RGS domain of regulator of G protein signaling 3 (RGS3). J Struct Biol 170, 451–461 (2010). [PubMed: 20347994]

28. Daumke O, Weyand M, Chakrabarti PP, Vetter IR, Wittinghofer A, The GTPase-activating protein Rap1GAP uses a catalytic asparagine. Nature 429, 197–201 (2004). [PubMed: 15141215]

29. Li Y, Inoki K, Guan KL, Biochemical and functional characterizations of small GTPase Rheb and TSC2 GAP activity. Mol Cell Biol 24, 7965–7975 (2004). [PubMed: 15340059]

30. Sunaga N et al. , Knockdown of oncogenic KRAS in non-small cell lung cancers suppresses tumor growth and sensitizes tumor cells to targeted therapy. Mol Cancer Ther 10, 336–346 (2011). [PubMed: 21306997]

31. Gibbs JB, Schaber MD, Allard WJ, Sigal IS, Scolnick EM, Purification of ras GTPase activating protein from bovine brain. Proc Natl Acad Sci U S A 85, 5026–5030 (1988). [PubMed: 3293047]

32. Webb MR, A continuous spectrophotometric assay for inorganic phosphate and for measuring phosphate release kinetics in biological systems. Proc Natl Acad Sci U S A 89, 4884–4887 (1992). [PubMed: 1534409]

33. Lito P et al. , Disruption of CRAF-mediated MEK activation is required for effective MEK inhibition in KRAS mutant tumors. Cancer Cell 25, 697–710 (2014). [PubMed: 24746704]

34. Waters AM et al. , Evaluation of the selectivity and sensitivity of isoform- and mutation-specific RAS antibodies. Sci Signal 10, (2017).

35. Bankhead P et al. , QuPath: Open source software for digital pathology image analysis. Sci Rep 7, 16878 (2017). [PubMed: 29203879]

36. Xue Y et al. , An approach to suppress the evolution of resistance in BRAF(V600E)-mutant cancer. Nat Med 23, 929–937 (2017). [PubMed: 28714990]

37. Hofmann MH et al. , BI-3406, a Potent and Selective SOS1-KRAS Interaction Inhibitor, Is Effective in KRAS-Driven Cancers through Combined MEK Inhibition. Cancer Discov 11, 142–157 (2021). [PubMed: 32816843]
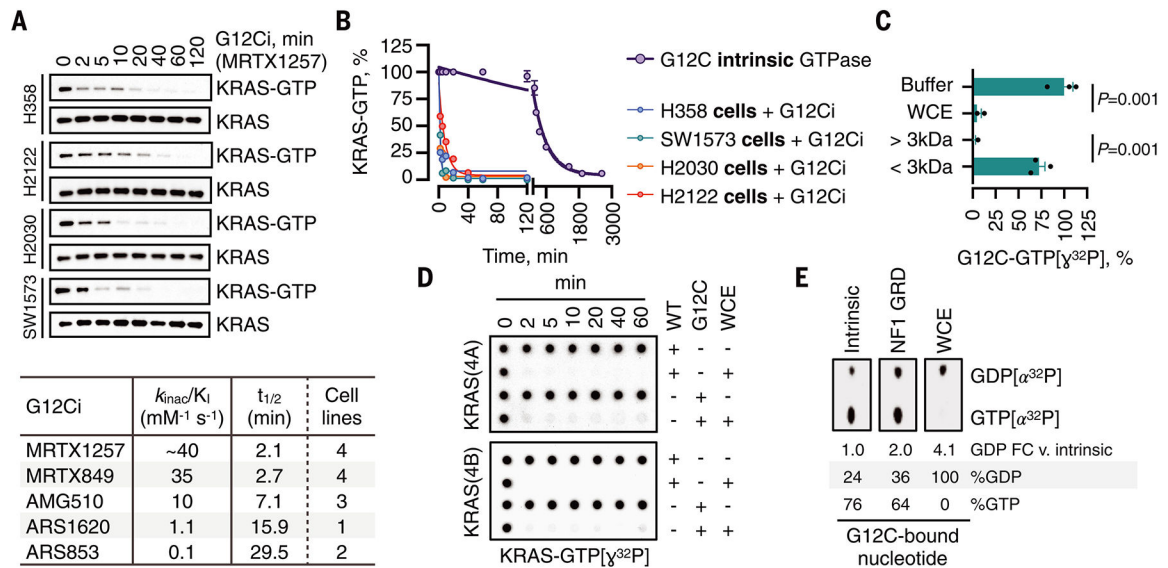
Fig. 1. Cancer cell extracts enhance the GTPase activity of KRAS^{G12C}.

(**A**) KRAS^{G12C}-mutant cell lines were serum-deprived for 16 h and treated as shown. The level of active KRAS (GTP-bound) was determined by RAS-binding domain (RBD)-pulldown and quantified by densitometry. Bottom: The potency of drug binding to G12C (k_{inac}/K_I) and the half-life for cellular inhibition (mean from the indicated number of cell lines). (**B**) KRAS^{G12C} was loaded with GTP[γ^{32}P] and its intrinsic GTPase activity was assayed over time, ensuring sufficient time for the reaction to reach completion (mean ± s.e.m, n=2). Also shown is the effect of MRTX1257 treatment on the ratio of active to total cellular KRAS. (**C**) GTP[γ^{32}P] hydrolysis by KRAS^{G12C} was assayed in the absence or presence of whole-cell extracts (WCE) from H358 lung cancer cells (mean ± s.e.m, n=3, two-tailed p value). WCE were either added directly or after fractionation with a 3 kDa molecular cut-off column. (**D**) KRAS splice variants 4A or 4B, either WT or G12C mutant, were loaded with GTP[γ^{32}P] and assayed for GTP-hydrolysis over time. (**E**) Thin layer chromatography (TLC) was used to separate α^{32}P-labeled nucleotides that were eluted from KRAS^{G12C} incubated with the NF1 GAP-related domain (GRD) or H358 cellular extracts. Shown are the fold increase in the absolute GDP[α^{32}P] signal and the percent α^{32}P-labeled nucleotide relative to the total signal per sample. FC: fold change. A representative of at least two experimental repeats is shown in D and E.
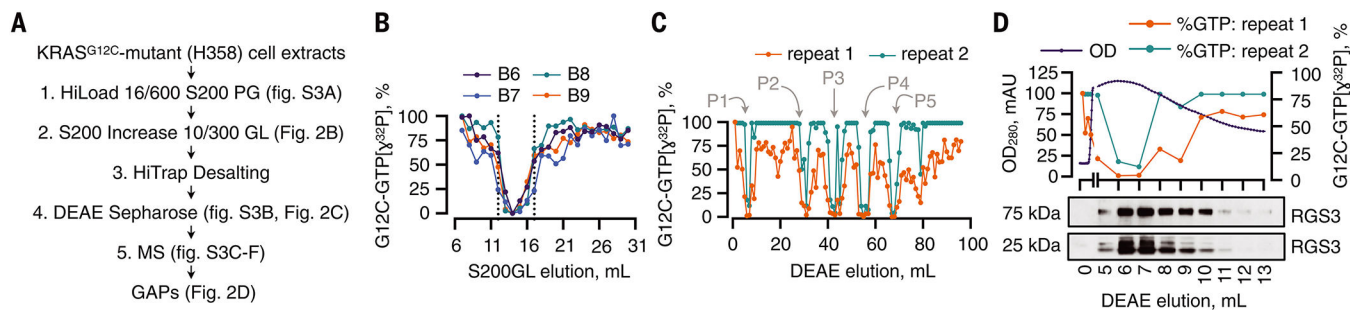
Fig. 2. Identification of a protein that enhances the GTPase activity of KRAS^{G12C}.
(**A**) The purification schema included size-exclusion chromatography (SEC, steps 1 and 2), desalting (step 3), anion-exchange chromatography (AEC, step 4) and mass spectrometry (MS, step 5). (**B**) H358 cell extracts (2 g) were subjected to SEC and eluted fractions (1 mL each) were incubated with GTP[γ^{32}P]-loaded KRAS^{G12C} for 1 h and subjected to the γ-phosphate assay. The G12C-GTP[γ^{32}P] signal in each fraction from step 2 is shown. See fig. S3A for step 1 analysis. (**C**) Active fractions from step 2 (12–17 mL) were pooled, desalted and subjected to AEC using a linear salt-gradient. The effect of each fraction on GTPase activity is shown. See also fig. S3B. (**D**) The elution of RGS3 p75 and p25 variants in fractions from peak 1 (P1) and the effect on KRAS^{G12C} GTPase activity.
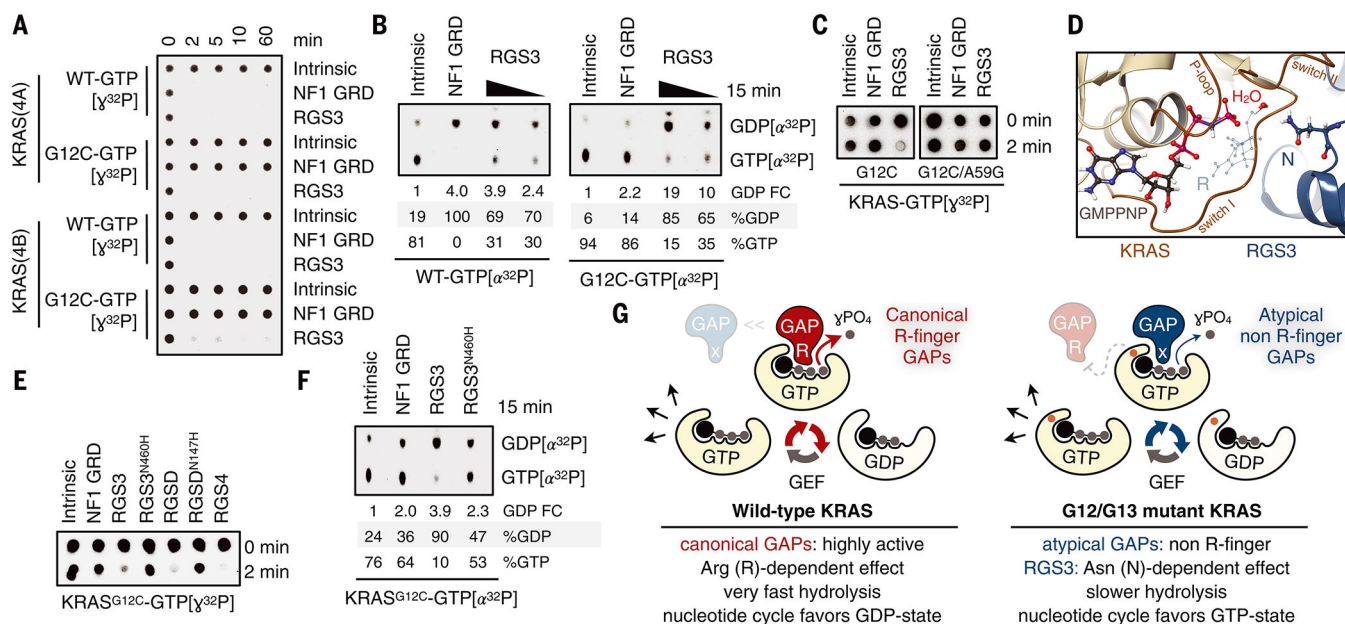
Fig. 3. Mechanistic basis for RGS3-assisted GTP-hydrolysis by KRAS^{G12C}.
(**A**, **B**) GTP[γ^{32}P]-loaded KRAS variants were incubated with buffer, NF1 GAP-related domain (GRD) or RGS3 (p75) for the indicated times, followed by determination of GTPase activity by using the γ-phosphate assay (A) or the α-phosphate assay (B). (**C**) As in A, except that the hydrolysis transition-state mutation A59G was engineered alongside G12C. (**D**) Molecular model of the interaction of KRAS-GMPPNP with the GAP-domain of RGS3 (RGSD). The catalytic arginine residue of RASA1 (R) is superimposed as a reference point (not part of the modeling). (**E**, **F**) KRAS^{G12C} was loaded with GTP[γ^{32}P] (E) or GTP[α^{32}P] (F) and then incubated with WT or asparagine-to-histidine (NH) mutant RGS3 followed by determination of GTPase activity using the γ-phosphate (E) or the α-phosphate (F) assay. A representative of at least two experimental repeats is shown in A-C, E and F. (**G**) Schematic of the mechanism that enables mutant KRAS-inclusive GAP activity.
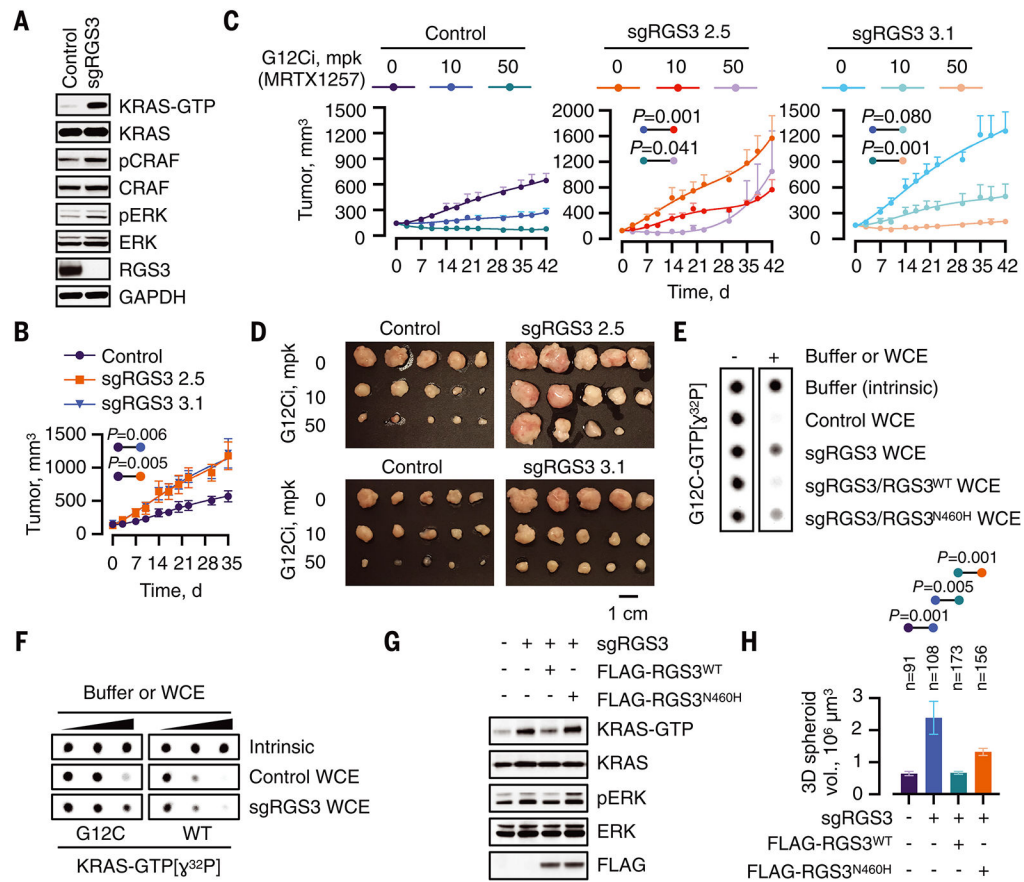
Fig. 4. RGS3 diminishes KRAS^{G12C} activation in cancer cells.

(**A**) WCE from control or RGS3-null H358 cells were immunoblotted to determine the effect on the indicated signaling intermediates. A representative of at least three experimental repeats is shown. (**B**) Control or RGS3$^{-/-}$ clones were implanted in athymic mice to determine the effect on tumor growth (n=10 for control and n=5 for each sgRGS3 clone). Mean ± s.e.m and two-tailed p values are shown. (**C**, **D**) Mice bearing control or RGS3$^{-/-}$ xenografts were treated as shown to determine the effect on tumor growth (n=10 for the control and n=5 for each sgRGS3 clone). Two-tailed p values (C) and endpoint tumor volumes (D) are shown. (**E**) Purified KRAS^{G12C} was loaded with GTP[γ^{32}P] and assayed for GTP-hydrolysis in the absence or presence of extracts (0.4 μg/μL) from control and RGS3$^{-/-}$ cells as well as extracts from RGS3$^{-/-}$ cells engineered to re-express WT or N460H mutant RGS3. (**F**) Purified KRAS^{WT} or KRAS^{G12C} proteins were loaded with GTP[γ^{32}P] and assayed for hydrolysis in the absence (intrinsic) or in the presence of extracts (WCE) from control or RGS3$^{-/-}$ cells (0, 0.1, 0.2 μg/μL). (**G**) WCE from the indicated cell lines were evaluated by RBD-pulldown to determine the amount of active KRAS. (**H**) The cells were cultured as 3D tumor spheroids in collagen I-containing medium for 17 days. The spheroid volumes were determined from representative images.